Chinese Chemical Letters 36 (2025) 109943

Contents lists available at ScienceDirect

Chinese Chemical Letters

journal homepage: www.elsevier.com/locate/cclet

Cationic covalent organic framework nanocarriers integrating both efficient gene silencing and real-time gene detection

Ziqin Li[a], Kai Hao[a], Longwei Xiang[a], Huayu Tian[a,b,c,*]

[a] State Key Laboratory of Physical Chemistry of Solid Surfaces, College of Chemistry and Chemical Engineering, Xiamen University, Xiamen 361005, China
[b] Innovation Laboratory for Sciences and Technologies of Energy Materials of Fujian Province (IKKEM), Xiamen 361005, China
[c] Changchun Institute of Applied Chemistry, Chinese Academy of Sciences, Changchun 130022, China

ARTICLE INFO

Article history:
Received 12 March 2024
Revised 24 April 2024
Accepted 28 April 2024
Available online 29 April 2024

Keywords:
Tumor diagnosis
Cancer therapy
Nucleic acid delivery
Cationic COF
Gene silencing

ABSTRACT

The occurrence, development, and metastasis of tumors often entail abnormal expression of genetic substances. Monitoring and regulating changes in intracellular nucleic acid substances hold promise for achieving accurate tumor diagnosis and effective treatment. However, the effectiveness of integrated tumor diagnosis and treatment based on functional nucleic acids still needs to be improved. In this study, we engineered a multifunctional nucleic acid delivery system grounded in a cationic covalent organic framework carrier. This system not only showcases effective gene silencing but also boasts high sensitivity in detecting miR21 levels within tumor cells, enabling real-time monitoring of tumor gene therapy efficacy. The construction of this integrated functional nucleic acid delivery platform provides new ideas for precise tumor detection and effective tumor treatment.

The occurrence, development and metastasis of tumor were often accompanied by changes in genetic substances [1,2]. After understanding the biological and molecular mechanisms of tumor occurrence, effective cancer therapy can be achieved by regulating the expression levels of tumor related genes in cancer cells. In addition, monitoring the expression level of cancer-related genes in cancer cells was useful for guiding precise cancer therapy [3]. Therefore, nucleic acid-based tumor diagnosis and therapy had an important position in the field of antitumor therapy

The effectiveness of nucleic acid-based tumor diagnosis and therapy hinges on delivering functional nucleic acids to specific locations within cells. But naked nucleic acids were easily degraded and difficult to enter cells effectively. Therefore, the nucleic acid delivery process often required the participation of nucleic acid carriers. Common nucleic acid delivery carriers for gene therapy included viruses [4], polyethylenimine (PEI) [5,6], polylysine (PLL) [7], dendrimers (PAMAM) [8], and liposomes [9]. Although these gene carriers had been extensively developed in the past few decades, it was still a challenge to obtain safe and efficient ones through simple methods. In addition to gene therapy, chemically modified nucleic acid substance could also be used to detect the content of miRNA. Realizing real-time nucleic acid detection in cells and tumor tissues was of great significance for tumor prevention and treatment, but it was also extremely challenging. With the aid of nucleic acid probe carrier, it was expected to achieve this goal. Common nucleic acid probe carriers mainly included gold nanoparticles (Au NPs) [10], manganese dioxide (MnO_2) nanosheets [11], graphene oxide (GO) [12], and upconversion nanoparticles (UCNPs) [13]. Most of them had the performance of quenching fluorescent groups, which could realize the visual detection of target nucleic acid substances. However, the biological safety of these nucleic acid delivery carriers and the detection sensitivity of target nucleic acids still need to be improved.

Covalent organic framework (COF) was a new class of porous materials. In recent years, it had been widely used in the field of biomedicine, such as chemotherapy, photodynamic therapy, and photothermal therapy [14]. It had been found that the cation-π interaction and porous structure help nanomaterials to adsorb nucleic acid species [15,16]. Therefore, some researchers had explored the application of COF in the field of nucleic acid delivery [17,18]. However, it was still limited by the larger size and poor dispersion of COF.

Based on the above researches and the foundation of our previous work [19], we had built a multifunctional nucleic acid delivery platform. Cationic covalent organic framework nanoparticles (LZU-Cys-NPs) with uniform and suitable size were prepared by using 1,3,5-benzenetricarboxaldehyde, *N*-Boc-*p*-phenylenediamine and cystamine hydrochloride as raw materials in a one-step process. The prepared LZU-Cys-NPs had the following advantages:

* Corresponding author.
E-mail address: thy@xmu.edu.cn (H. Tian).

https://doi.org/10.1016/j.cclet.2024.109943
1001-8417/

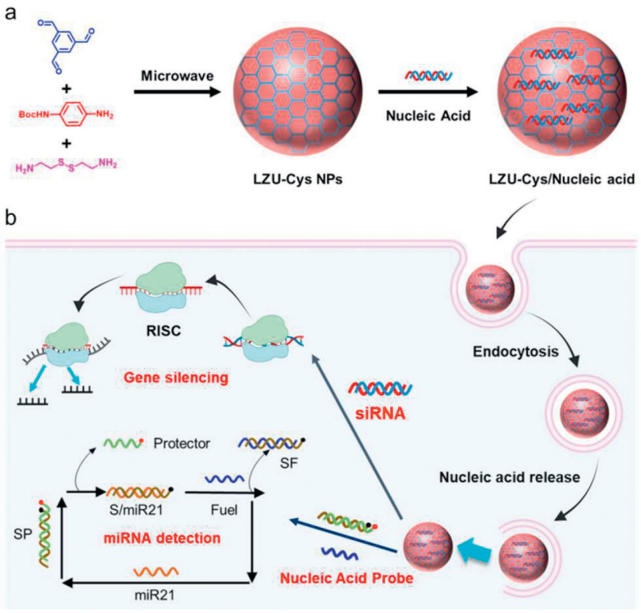

Scheme 1. Schematic diagram of the preparation and application of LZU-Cys-NPs. (a) The preparation process of LZU-Cys-NPs. (b) The process of gene silencing and miRNA detection.

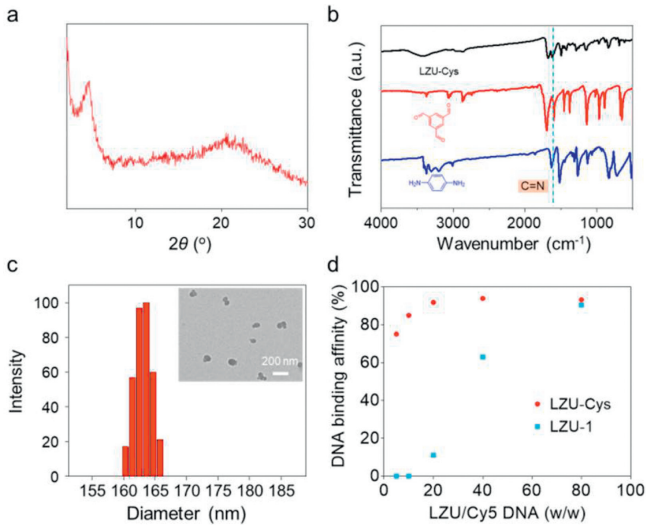

Fig. 1. (a) PXRD of LZU-Cys-NPs. (b) FTIR of 1,3,5-benzenetricarboxaldehyde, *p*-phenylenediamine and LZU-Cys-NPs. (c) DLS and TEM image of LZU-Cys-NPs. (d) Adsorption curve of Cy5-DNA on LZU-Cys-NPs and LZU-1 NPs.

(1) The preparation method of LZU-Cys-NPs was simple, and had uniform size and good dispersibility in water; (2) The prepared cationic COF nanoparticles had excellent gene silencing effect; (3) LZU-Cys-NPs could effectively adsorb nucleic acid probes for sensitive intracellular nucleic acid detection; (4) For the first time, we used modified COF to achieve efficient gene silencing and real-time gene detection.

The preparation of LZU-Cys-NPs was shown in Scheme 1. The powder X-ray diffraction (PXRD) results of LZU-Cys-NPs showed a sharp peak around 4°, indicating that the material had good crystallinity (Fig. 1a). The Fourier transform infrared absorption spectroscopy (FTIR) showed a new peak at 1603 cm^{-1}, indicating that the COF monomers were connected by C=N bonds (Fig. 1b). The dynamic light scattering (DLS) results showed that the size of LZU-Cys-NPs was about 160 nm, and transmission electron microscope (TEM) image showed that the nano-particles were regular and uniform in size (Fig. 1c). The zeta potential results showed that COFs doped with cysteamine had higher positive charges (Fig. S1 in Supporting information). The above results indicated the successful preparation of LZU-Cys-NPs, and it had good crystallinity and suitable size.

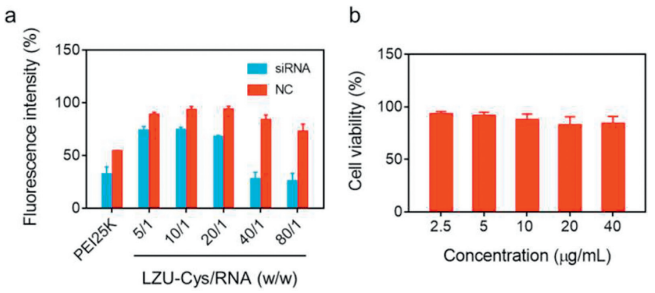

Fig. 2. (a) Gene silence efficiency of LZU-Cys-NPs in MCF-7-Luc cells. NC: non-coding RNA. (b) Cell viability of LZU-Cys-NPs. Data are presented as mean ± standard deviation (SD) ($n = 3$).

Excellent nucleic acid adsorption capacity was the basic performance of nucleic acid delivery carriers, so we first verified the adsorption capacity of LZU-Cys-NPs to Cy5-DNA. It could be seen from Fig. 1d that with the increased of material concentration, the ability of LZU-1 NPs and LZU-Cys-NPs to adsorb DNA gradually increased, and the adsorption efficiency could reach more than 90%. However, when the mass ratio of LZU-1 NPs to Cy5-DNA was 20/1, only 11% of DNA could be effectively adsorbed. However, under the same conditions, LZU-Cys-NPs had more than 85% of the adsorption efficiency of Cy5-DNA. This indicated that cation-modified COF NPs was excellent in nucleic acid adsorption.

In addition, we found that LZU-Cys-NPs also showed more prominent advantages than pure cationic polymers when carrying nucleic acid substances. Cationic polymers could carry nucleic acid substances through electrostatic interactions, but the particle size and morphology of the formed composite particles were greatly affected by the compounding conditions, polymer type and concentration, and the process repeatability was poor. In the nucleic acid delivery system we designed, when LZU-Cys-NPs were loaded with DNA, its particle size hardly changed, indicating that its structure had maintained good integrity. Moreover, it had good stability no matter in aqueous solution or 10% fetal bovine serum (FBS) solution (Figs. S2 and S3 in Supporting information).

After discovering that LZU-Cys-NPs could effectively adsorb nucleic acids, we continued to evaluate its gene delivery ability. First, luciferase-silencing siRNA was used as the reporter gene, and gene silencing experiments were performed in MCF-7-Luc cells. As could be seen from Fig. 2a, the control group PEI25K had 50% silencing efficiency. When LZU-Cys-NPs was at a low concentration, the gene silencing effect was not ideal, but as the concentration increased, the efficiency of gene silencing also increased significantly. LZU-Cys-NPs could achieve about 70% gene silencing efficiency at a mass ratio of 40/1 (Fig. 2a). However, it could be seen from Fig. 2b that even at a concentration of 40 μg/mL, LZU-Cys-NPs still had low cytotoxicity, which indicated that the prepared LZU-Cys-NPs was a safe and efficient gene carrier.

After finding that LZU-Cys-NPs had good gene silencing effect, we further constructed a miR21 detection platform based on LZU-Cys-NPs. We used the previously constructed FIRE nucleic acid probe for nucleic acid detection, and its working principle was shown in Fig. S4 (Supporting information) [20]. LZU-Cys/SPF nanocomposite was obtained by mixing SP DNA and Fuel DNA with LZU-Cys-NPs. The specific nucleic acid sequence was showed in Table S1 (Supporting information). After LZU-Cys-NPs and nucleic acid probes were evenly mixed, different amounts of miR21 were

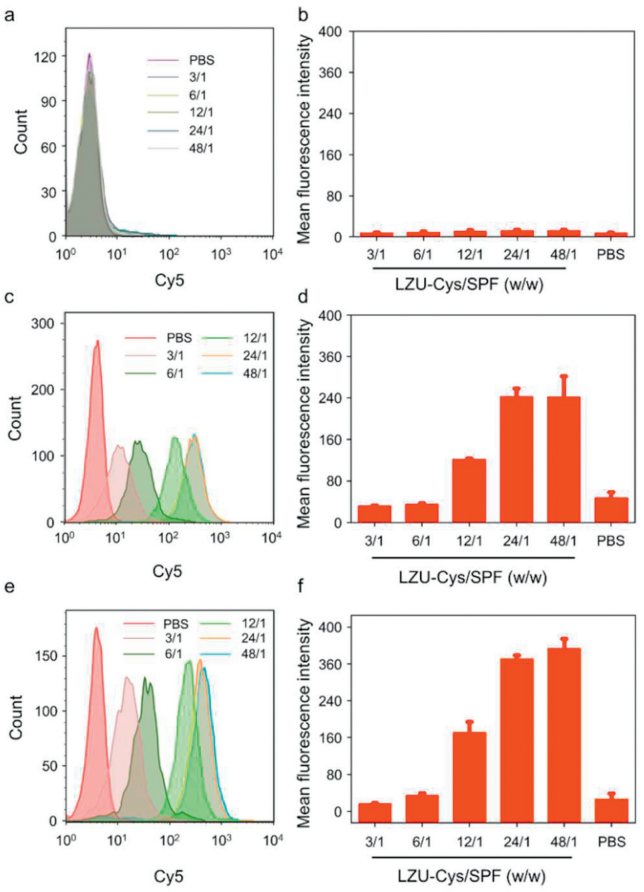

Fig. 3. (a, c, e) Detection of miR21 in CHO, HeLa, and MCF-7 cells incubated with LZU-Cys/SPF by flow cytometry and the mean fluorescence intensity of CHO (b), HeLa (d), and MCF-7 (f) cells. Data are presented as mean ± SD ($n = 3$).

added, and finally the fluorescence intensity of the solution was measured. It could be seen from Fig. S5a (Supporting information) that as the amount of miR21 increased, the fluorescence intensity of the solution gradually increased. Further, when the miR21 concentration was from 0.05 nmol/L to 2 nmol/L, the fluorescence intensity had a good linear relationship (Fig. S5b in Supporting information). Based on this, we measured the limit of detection (LOD) of miR21 on the LZU-Cys/SPF detection platform, and the LOD value obtained was 9.37 pmol/L.

Then we used LZU-Cys/SPF to detect the content of miR21 in CHO, HeLa, and MCF-7 cells, respectively. From Fig. 3, it could be found that the fluorescence signal in CHO cells was the weakest, the fluorescence signal in HeLa cells was stronger, and the fluorescence signal in MCF-7 was the strongest, and there was a significant difference among them (Fig. S6 in Supporting information). This indicated that our miR21 detection system could distinguish between normal cells and cancer cells depending on the fluorescence intensity. In addition, we could see that in the three types of cells, as the mass ratio of LZU-Cys-NPs to SPF increased, the intracellular fluorescence signal gradually increased and reached a maximum value around 24/1. This was consistent with the ability of LZU-Cys-NPs to adsorb nucleic acids. From the confocal laser microscope (CLSM) images, the level of miR21 content in different cells could be seen more intuitively. As shown in Fig. S7 (Supporting information), we could clearly see the difference in miR21 content in CHO, HeLa and MCF-7 cells, which was consistent with the results of flow cytometry.

After verifying that LZU-Cys-NPs has good gene silencing and gene detection effects, we used LZU-Cys-NPs to perform gene regulation and real-time gene detection experiments on MCF-7 cells (Fig. 4). In the positive group, LZU-Cys-NPs were first used to deliver miR21 mimics into cells, which is a single-stranded DNA with the same sequence as miR21. This mimics increased expression of miR21 in the cell. In the negative group, LZU-Cys-NPs were first used to deliver anti-miR21 into cells, which had the ability to silence miR21. In the control group, the cells underwent the same treatment, except that the vector/nucleic acid complex solution was replaced with an equal amount of PBS. After 6 h of the above-mentioned treatment on the cells, LZU-Cys-NPs were used to carry nucleic acid probes for nucleic acid detection of the cells, and the detection results were observed by CLSM. From Fig. 4, we could see that after treatment with LZU-Cys/anti-miR21, the red fluorescence of the cells was significantly reduced, while strong red fluorescence could be observed in MCF-7 cells treated with PBS. In addition, the cells treated with the LZU-Cys/miR21 mimic had the strongest red fluorescence. Because LZU-Cys/anti-miR21 could reduce the number of miR21 in MCF7 cells, while the LZU-Cys/miR21 mimic could increase the number of miR21 in cells. These results indicated that LZU-Cys-NPs could not only effectively deliver miR21 mimics or anti-miR21 to cells, but also could evaluate the delivery effect of nucleic acids in real time after SPF was loaded.

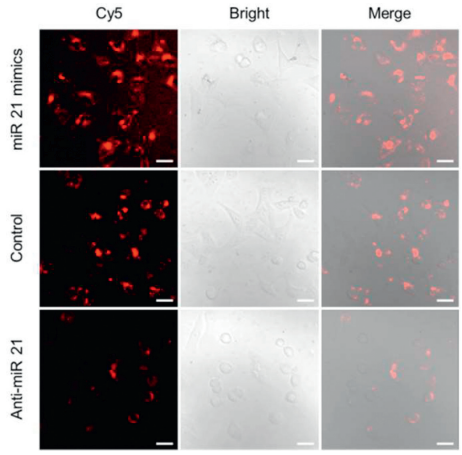

Fig. 4. CLSM images of MCF-7 cells pretreated with LZU-Cys/miR21 mimics, PBS and LZU-Cys/anti-miR21, followed by exposure to LZU-Cys/SPF. Scale bar: 20 μm.

In summary, based on LZU-Cys-NPs with uniform size and good dispersion, we had constructed a multifunctional nucleic acid delivery platform. The prepared LZU-Cys-NPs showed excellent nucleic acid adsorption capacity and good biocompatibility. The cell-level gene silencing experiment results showed that the prepared nanoparticles had an excellent gene silencing effect. Moreover, after loading oligonucleotide probes, fluorescence analysis could not only distinguish normal cells from tumor cells, but also observed the silencing effect of miR21 in real time. It was understood that this was the first use of a nucleic acid delivery platform based on COF nanoparticles to achieve efficient gene silencing and real-time gene detection at the level of living cells, which provided a new strategy for the realization of precise gene therapy in the future.

Declaration of competing interest

The authors declare that they have no known competing financial interests or personal relationships that could have appeared to influence the work reported in this paper.

CRediT authorship contribution statement

Ziqin Li: Writing – review & editing, Writing – original draft, Visualization, Validation, Investigation, Data curation, Conceptual-

ization. **Kai Hao:** Writing – review & editing, Visualization, Validation, Investigation, Data curation, Conceptualization. **Longwei Xiang:** Data curation. **Huayu Tian:** Writing – review & editing, Supervision, Resources, Funding acquisition, Conceptualization.

Acknowledgments

The authors are thankful to the National Key Research and Development Program of China (No. 2021YFB3800900), National Natural Science Foundation of China (No. 51925305), and the talent cultivation project Funds for the Innovation Laboratory for Sciences and Technologies of Energy Materials of Fujian Province (No. HRTP-[2022]52).

Supplementary materials

Supplementary material associated with this article can be found, in the online version, at doi:10.1016/j.cclet.2024.109943.

References

[1] L.G.T. Morris, T.A. Chan, Cancer 121 (2015) 1357–1368.
[2] T. Friedmann, Cancer 70 (1992) 1810–1817.
[3] P.L. Patel, N.K. Rana, M.R. Patel, S.D. Kozuch, D. Sabatino, ChemMedChem 11 (2016) 252–269.
[4] Y.Z. Liu, A. Deisseroth, Blood 107 (2006) 3027–3033.
[5] C. Xu, H. Tian, Y. Wang, et al., Chin. Chem. Lett. 28 (2017) 807–812.
[6] L. Lin, Z.P. Guo, J. Chen, H.Y. Tian, X.S. Chen, Acta. Polym. Sin. 16277 (2017) 321–328.
[7] H. Fang, Z. Guo, L. Lin, et al., J. Am. Chem. Soc. 140 (2018) 11992–12000.
[8] Y. Wang, C. Li, L. Du, Y. Liu, Chin. Chem. Lett. 31 (2020) 275–280.
[9] R. Suzaki, T. Takizawa, Y. Negishi, et al., J. Control. Release 125 (2008) 137–144.
[10] J. Wang, C. Wang, J. Xu, X. Xia, H. Chen, Chin. Chem. Lett. 34 (2023) 108165.
[11] S. Wang, L. Wang, X. Xu, X. Li, W. Jiang, Anal. Chim. Acta 1063 (2019) 152–158.
[12] L. Yang, J. Li, W. Pan, et al., Chem. Commun. 54 (2018) 3656–3659.
[13] G. Wang, Y. Fu, Z. Ren, et al., Chem. Commun. 54 (2018) 6324–6327.
[14] H. Wei, X. Li, F. Huang, et al., Chin. Chem. Lett. 34 (2023) 108564.
[15] C. He, M. Wang, X. Sun, et al., Biosens. Bioelectron. 129 (2019) 50–57.
[16] S. Peng, B. Bie, Y. Sun, et al., Nat. Commun. 9 (2018) 1293.
[17] Y. Shi, J. Yang, F. Gao, Q. Zhang, ACS Nano 17 (2023) 1879–1905.
[18] Y. Cao, J. Zhang, L. Wang, et al., ACS Appl. Nano Mater 4 (2021) 4948–4955.
[19] K. Hao, Z. Guo, L. Lin, et al., Sci. China Chem. 64 (2021) 1235–1241.
[20] N. Yan, X. Wang, L. Lin, et al., Adv. Funct. Mater. 28 (2018) 1800490.